J|A|C|S
ARTICLES
Published on Web 08/17/2007

Using Measurements of Anchoring Energies of Liquid Crystals on Surfaces To Quantify Proteins Captured by Immobilized Ligands

Thimmaiah Govindaraju,[†,‡] Paul J. Bertics,[§] Ronald T. Raines,*[,‡] and Nicholas L. Abbott*[,†]

Contribution from the Departments of Chemical and Biological Engineering, Biomolecular Chemistry, Biochemistry, and Chemistry, University of Wisconsin-Madison, Madison, Wisconsin 53706

Received May 6, 2007; E-mail: abbott@engr.wisc.edu; raines@biochem.wisc.edu

Abstract: We describe a simple optical method that employs measurement of the interaction energy of a liquid crystal (LC) with a surface (the so-called anchoring energy) to report proteins captured on surfaces through specific interactions with immobilized binding groups. To define the sensitivity and dynamic range of the response of the LC, we covalently immobilized a tyrosine-containing, 13-residue peptide sequence (**Y1173**) from the epidermal growth factor receptor/kinase (EGFR) at which autophosphorylation takes place and to which the adapter protein Shc binds. We determined that, on peptide-decorated (**Y1173** or **pY1173**, where **pY1173** is the corresponding phosphopeptide) surfaces incubated against anti-phosphotyrosine antibody, the anchoring energy of the LC decreased systematically from 4.4 to 1.4 μJ/m^2 (with SEM = 0.3 μJ/m^2 for $n = 5$) as the antibody concentration increased from 10 pM to 100 nM. Over the same range of antibody concentrations in solution and densities of immobilized peptides, independent ellipsometric measurements were not sufficiently sensitive to report the captured antibody (ellipsometric thicknesses were $<$0.1 nm). These results, when combined with control experiments reported in this article, provide the first demonstration of the use of anchoring energy measurements of LCs to report proteins captured by immobilized ligands on surfaces. The sensitivity and dynamic range of the methodology suggest that it may offer the basis of a simple yet broadly useful principle for reporting the interactions between proteins and other biomolecules that underlie complex and poorly understood chemical and biological events.

Introduction

The development of simple and general methods that permit direct reporting of specific proteins captured by binding groups patterned on surfaces represents a largely unsolved challenge.[1] Mass spectroscopy[2a,b] and evanescent optical methods such as surface plasmon resonance[2c−e] are promising approaches but suffer from reliance on relatively complex instrumentation. Approaches that require redox-active,[3] fluorescent,[3,4a] or radioactive labels[4b,c] have the advantage of not requiring complex equipment but possess other disadvantages such as requiring multiple binding steps and secondary antibodies.[1,3,4a] In this article, we describe a method that permits direct reporting of proteins captured on surfaces by quantifying the energy of interaction of liquid crystals (LCs) with surfaces. The method is relatively simple to perform, does not require complex instrumentation or labels, and is demonstrated in this article to be useful for reporting proteins captured using oligopeptides patterned on surfaces.

The approach described in this article revolves around the orientational behavior of liquid crystalline materials at surfaces.[5−7] A very large number of past studies have demonstrated that the orientational ordering of micrometer-thick films of LCs supported on surfaces is remarkably sensitive to the nanoscopic topography and chemical functionality of surfaces.[8−21] Mini-

[†] Department of Chemical and Biological Engineering.
[‡] Departments of Biochemistry and Chemistry.
[§] Department of Biomolecular Chemistry.

(1) (a) Phizicky, E.; Bastiaens, P. I.; Zhu, H.; Snyder, M.; Fields, S. *Nature* **2003**, *422*, 208−215. (b) MacBeath, G. *Nat. Genet.* **2002**, *32*, 526−532.
(2) (a) Min, D.-H.; Su, J.; Mrksich, M. *Angew. Chem., Int. Ed.* **2004**, *43*, 5973−5977. (b) Su, J.; Rajapaksha, T. W.; Peter, M. E.; Mrksich, M. *Anal. Chem.* **2006**, *78*, 4945−4951. (c) Houseman, B. T.; Huh, J. H.; Kron, S. J.; Mrksich, M. *Nat. Biotechnol.* **2002**, *20*, 270−274. (d) McDonnell, J. M. *Curr. Opin. Chem. Biol.* **2001**, *5*, 572−577. (e) Stenlund, P.; Babcock, G. J.; Sodroski, J.; Myszka, D. G. *Anal. Biochem.* **2003**, *316*, 243−250.
(3) (a) Kirka, L. J. *Clin. Chem.* **1999**, *45*, 453−458. (b) Simeonov, A.; Bi, X.; Nikiforov, T. T. *Anal. Biochem.* **2002**, *304*, 193−199. (c) Liotta, L. A.; Espina, V.; Mehta, A. I.; Calvert, V.; Rosenblatt, K.; Geho, D.; Munson, P. J.; Young, L.; Wulfkuhle, J.; Petricoin, E. F. *Cancer Cell* **2003**, *3*, 317−325. (d) Paweletz, C. P.; Charboneau, L.; Bichsel, V. E.; Simone, N. L.; Chen, T.; Gillespie, J. W.; Emmert-Buck, M. R.; Roth, M. J.; Petricoin, I. E.; Liotta, L. A. *Oncogene* **2001**, *20*, 1981−1989.
(4) (a) Martinez, M. J.; Aragon, M. D.; Rodriguez, A. L.; Weber, J. M.; Timlin, J. A.; Sinclair, M. B.; Haaland, D. M.; Werner-Washburne, M. *Nucleic Acid Res.* **2003**, *31*, e18. (b) Falsey, J. R.; Renil, M.; Park, S.; Li, S.; Lam, K. S. *Bioconjugate Chem.* **2001**, *12*, 346−353. (c) Zhu, H.; Klemic, J. F.; Chang, S.; Bertone, P.; Casamayor, A.; Klemic, K. G.; Smith, D.; Gerstein, M.; Reed, M. A.; Snyder, M. *Nat. Genet.* **2000**, *26*, 283−289.
(5) Jerome, B. *Rep. Prog. Phys.* **1991**, *54*, 391−451.
(6) de Gennes, P. G. *The Physics of Liquid Crystals*, 1st ed.; Oxford University Press: London, 1974.
(7) Cognard, J. *Mol. Cryst. Liq. Cryst. Suppl.* **1982**, *78*, 1−77.
(8) Toney, M. F.; Russell, T. P.; Logan, J. A.; Kikuchi, H.; Sands, J. M.; Kumar, S. K. *Nature* **1995**, *374*, 709−711.
(9) Stohr, J.; Samant, M. G.; Luning, J.; Callegari, A. C.; Chaudhari, P.; Doyle, J. P.; Lacey, J. A.; Lien, S. A.; Purushothaman, S.; Speidell, J. L. *Science* **2001**, *292*, 2299−2302.

mization of the free energy of interaction of a LC with a surface results in the LC adopting a preferred orientation at the surface. This preferred orientation, referred to as the "easy axis" of the LC (η_0), propagates far from the surface because of long-range orientational ordering of molecules within a liquid crystalline material.[15−19] The orientation of the easy axis of a LC is easily determined by the transmission of polarized light through the LC.[15−19] Among these past studies of the orientational ordering of LCs at surfaces is a series of articles that describe measurements of changes in the easy axes of LCs as a means of reporting proteins captured on surfaces.[22−28] The imaging of proteins captured on surfaces via protein−protein interactions,[22−26] protein−small molecule interactions,[27] and through use of affinity contact printing has been shown to be possible by using LCs.[28] In this article, we describe a study that sought to build from these past accomplishments to provide a methodology with increased sensitivity and the capability to report proteins over the wider range of concentrations, as compared to past studies.

The approach that we report in this article involves measurement of the energy of interaction of LCs with surfaces. The interaction energy of a LC with a surface, which is referred to hereafter as the anchoring energy, is determined by applying a mechanical torque of known magnitude to the LC and measuring the resulting response of the LC.[5,29,32] The response is reported as a deviation in the orientation of the LC from the easy axis (under the influence of the mechanical torque).[29,32] We recently reported use of this methodology to measure the anchoring energy of LCs at surfaces presenting biologically relevant chemical functionality such as oligomers of ethylene glycol[29] and oligopeptides.[30,31] The sensitivity of the method is illustrated by our previous observation that surfaces presenting trimers of ethylene glycol (**EG3**) were easily distinguished from surfaces presenting tetramers of ethylene glycol (**EG4**) by measurement of anchoring energies of LCs.[29]

The basis of the method is most easily understood by making reference to Figure 1. The surface to be characterized using the LC is assembled into an optical cell comprising the surface of interest (top surface in Figure 1) and a reference surface (bottom surface in Figure 1). These surfaces are designed (see below for details) such that a LC, when wicked into the cavity between the two surfaces, is twisted by angle ψ (typically 90°). The presence of the twist distortion within the LC generates a torque that acts on the surface of interest so as to displace the azimuthal orientation of the LC (η_d) from the easy axis (η_0) at that surface. Measurement of the azimuthal angular displacement, depicted as the angle φ in Figure 1, is straightforward to perform (requires rotation of a polarizer) and can be used to calculate the anchoring energy of the LC, W (with dimensions of energy per unit area), at the surface of interest.[32] Typical values of anchoring energies of LCs are in the 1−100 μJ/m^2 range.[29,30,32]

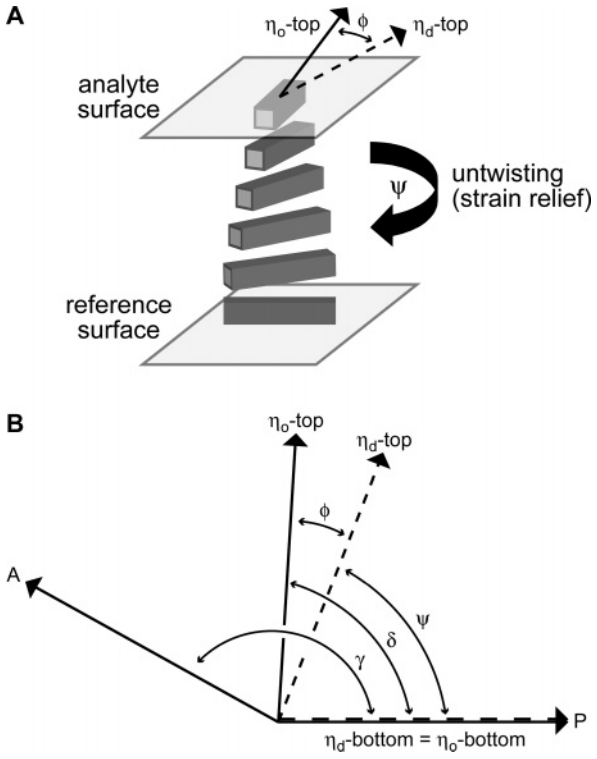

Figure 1. (A) Schematic illustration of modified torque balance method used to measure anchoring energies, where φ is deviation of director η_d from the easy axis η_0 and ψ is twist angle of the LC. (B) Angle diagram (see text for details). A: Analyzer. P: Polarizer.

For the study reported in this article, we used surfaces prepared by physical vapor deposition of thin gold films at an oblique (grazing) angle of incidence.[33] Gold films prepared in this manner are known to possess an in-plane structure (nanoscopic topography as well as in-plane crystallographic texture)[33] and can be used to support self-assembled monolayers (SAMs) formed from organothiol compounds. The structure of the gold film and organothiol combine to produce well-defined orientations of the easy axes of nematic LCs on these surfaces. The SAMs used in the current study were terminated with tetramers of ethylene glycol (to minimize nonspecific adsorption of proteins[34]) and were mixed with a small percentage of an amine-

(10) Seo, D.-S.; Muroi, K.; Isogami, T.; Matsuda, H.; Kobayashi, S. *Jpn. J. Appl. Phys., Part 1* **1992**, *31*, 2165−2169.
(11) Gibbons, W. M.; Shannon, P. J.; Sun, S.-T.; Swetlin, B. J. *Nature* **1991**, *351*, 49−50.
(12) Schadt, M.; Seiberle, H.; Schuster, A. *Nature* **1996**, *381*, 212−215.
(13) Janning, J. L. *Appl. Phys. Lett.* **1972**, *21*, 173−174.
(14) (a) Iwamoto, M.; Kato, K.; Matsumura, A.; Majima, Y. *Jpn. J. Appl. Phys.* **1999**, *38*, 5984−5990. (b) Ichimura, K. In *Polymer as Electrooptical and Photooptical Active Media;* Shibaev, V., Ed.; Springler: New York, 1997; pp 138−170. (c) Ichimura, K. *Chem. Rev.* **2000**, *100*, 1847−1874.
(15) Luk, Y.-Y.; Abbott, N. L. *Science* **2003**, *301*, 623−626.
(16) Brake, J. M.; Mezera, A. D.; Abbott, N. L. *Langmuir* **2003**, *19*, 8629−8637.
(17) Shah, R. R.; Abbott, N. L. *J. Am. Chem. Soc.* **1999**, *121*, 11300−11310.
(18) Shah, R. R.; Abbott, N. L. *J. Phys. Chem. B* **2001**, *105*, 4936−4950.
(19) Clare, B. H.; Efimenko, K.; Fischer, D. A.; Genzer, J.; Abbott, N. L. *Chem. Mater.* **2006**, *18*, 2357−2363.
(20) Berreman, D. W. *Phys. Rev. Lett.* **1972**, *28*, 1683−1686.
(21) Feller, M. B.; Chen, W.; Shen, Y. R. *Phys. Rev. A: At., Mol., Opt. Phys.* **1991**, *43*, 6778−6792.
(22) Gupta, V. K.; Skaife, J. J.; Dubrovsky, T. B.; Abbott, N. L. *Science* **1998**, *279*, 2077−2080.
(23) Skaife, J. J.; Abbott, N. L. *Langmuir* **2000**, *16*, 3529−3536.
(24) Skaife, J. J.; Abbott, N. L. *Langmuir* **2001**, *17*, 5595−5604.
(25) Skaife, J. J.; Brake, J. M.; Abbott, N. L. *Langmuir* **2001**, *17*, 5448−5457.
(26) Luk, Y.-Y.; Tingey, M. L.; Hall, D. J.; Israel, B. A.; Murphy, C. J.; Bertics, P. J.; Abbott, N. L. *Langmuir* **2003**, *19*, 1671−1680.
(27) Clare, B. H.; Abbott, N. L. *Langmuir* **2005**, *21*, 6451−6461.
(28) Jang, C.-H.; Tingey, M. L.; Korpi, N. L.; Wiepz, G. J.; Schiller, J. H.; Bertics, P. J.; Abbott, N. L. *J. Am. Chem. Soc.* **2005**, *127*, 8912−8913.
(29) Clare, B. H.; Guzman, O.; de Pablo, J. J.; Abbott, N. L. *Langmuir* **2006**, *22*, 4654−4659.
(30) Clare, B. H.; Guzman, O.; de Pablo, J. J.; Abbott, N. L. *Langmuir* **2006**, *22*, 7776−7782.
(31) Luk, Y.-Y.; Tingey, M. L.; Dickson, K. A.; Raines, R. T.; Abbott, N. L. *J. Am. Chem. Soc.* **2004**, *126*, 9024−9032.
(32) Fonseca, J. G.; Galerne, Y. *Appl. Phys. Lett.* **2001**, *79*, 2910−2912.
(33) Skaife, J. J.; Abbott, N. L. *Chem. Mater.* **1999**, *11*, 612−623.
(34) (a) Prime, K. L.; Whitesides, G. M. *Science* **1991**, *252*, 1164−1167. (b) Lahiri, J.; Isaacs, L.; Tien, J.; Whitesides, G. M. *Anal. Chem.* **1999**, *71*, 777−790. (c) Luk, Y.-Y.; Kato, M.; Mrksich, M. *Langmuir* **2000**, *16*, 9604−9608. (d) Kane, R. S.; Deschatelets, P.; Whitesides, G. M. *Langmuir* **2003**, *18*, 2388−2391.

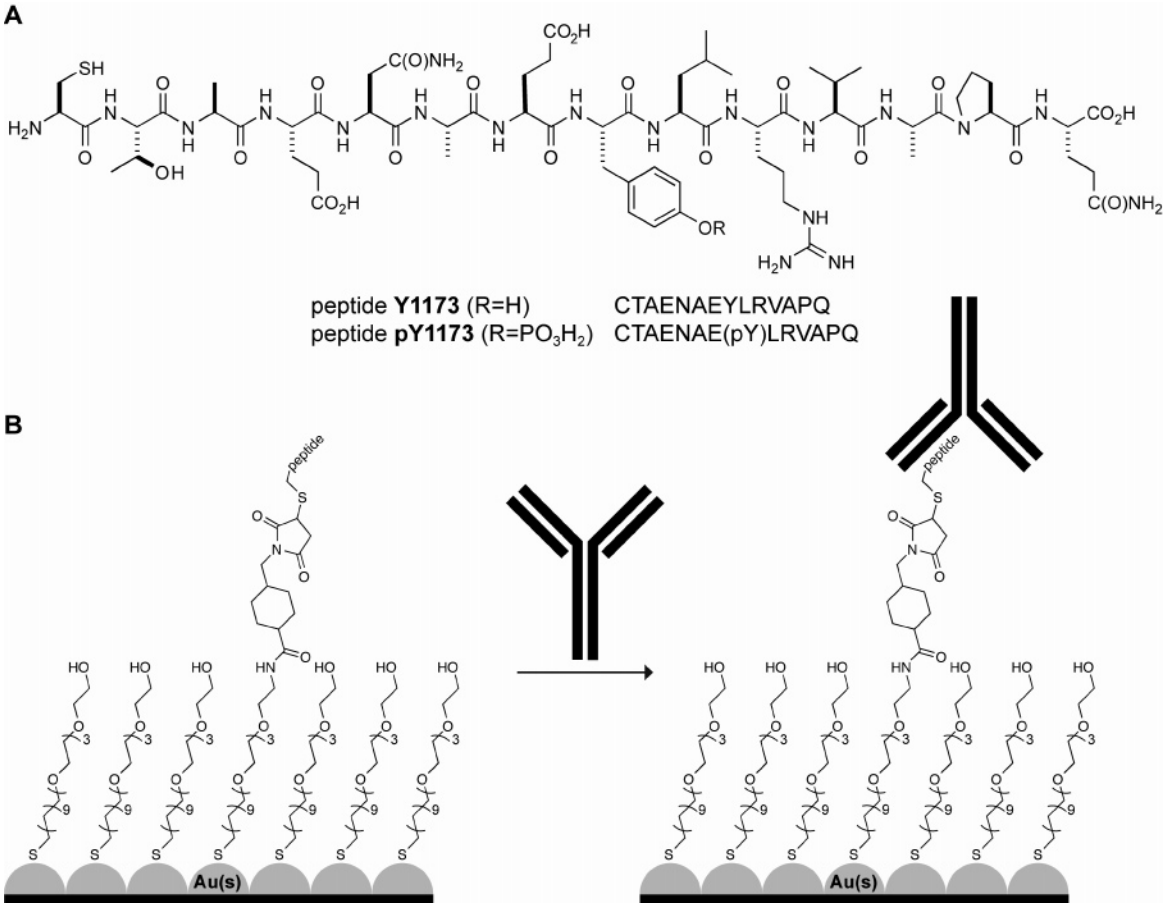

Figure 2. (A) Molecular structures of EGFR peptides **Y1173** and **pY1173**. (B) Schematic illustration of a gold film supported on a glass slide on which a mixed monolayer of **EG4** and **EG4N** is formed. The surface was activated using SSMCC to immobilize either **Y1173** or **pY1173**. The figure shows an antibody binding to the immobilized peptide.

terminated tetraethylene glycol to which oligopeptides were covalently attached using established methods (Figure 2).[27,30,31] The peptides immobilized in our study (denoted **Y1173** or **pY1173**, where the "p" denotes the phosphorylated peptide) were 13-residue peptides from the epidermal growth factor receptor (EGFR) (Figure 2A). EGFR is a transmembrane glycoprotein possessing EGF-stimulated tyrosine kinase activity, which in turn leads to intracellular substrate phosphorylation and self-phosphorylation.[35] The 13-residue peptide sequence used in our study comes from one of the major sites of self-phosphorylation (Tyr1173) of EGFR.[36,37] Once activated by phosphorylation, EGFR mediates the binding of the phosphotyrosine binding domain of Grb2 through direct interactions with Tyr1068 and Tyr1086 and through indirect interactions with Tyr1173.[38] Tyr1173 of EGFR also functions as a kinase substrate.[39]

In this article, we report measurements of the anchoring energies of LCs on surfaces decorated with EGFR peptide sequences **Y1173** and **pY1173** shown in Figure 2A following incubation of the surfaces against anti-phosphotyrosine antibodies which were expected to bind to **pY1173** but not **Y1173**. We elected to study anti-phosphotyrosine antibody binding to the EGFR peptides for two reasons. First, overproduction of wild-type and/or variant EGFR is associated with cancers having some of the worst prognoses.[40] The development of general and facile methods to detect very low concentrations of phosphorylated EGFR peptides on a surface will enable new methods for estimating the level of tyrosine kinase activity of EGFR. Such methods will be broadly useful for providing insights into molecular mechanisms underlying cancerous cellular states as well as for understanding the mechanisms of action of anticancer drugs targeted at EGFR.[35,40,41] Second, phosphorylation is an important physiological event that triggers numerous cellular signaling pathways.[35,40,41] The development of new tools for assessing regulation and activation of biomolecules such as EGFR will therefore be generalizable to analysis of a wide range of other protein kinases. The system under study can therefore also be viewed as a simple model of a broad class of important protein-binding interactions.

Materials and Methods

All materials were used as received unless otherwise noted. Fisher's Finest glass slides were obtained from Fisher Scientific (Pittsburgh, PA). Gold of 99.999% purity was obtained from International Advanced

(35) (a) Carpenter, G.; Cohen, S. *J. Biol. Chem.* **1990**, *265*, 7709−7712. (b) Ullrich, A.; Schlessinger, J. *Cell* **1990**, *61*, 203−212. (c) Bertics, P. J.; Gill, G. N. *J. Biol. Chem.* **1985**, *260*, 14642−14647.
(36) Batzer, A. G.; Rotin, D.; Urena, J. M.; Skolnik, E. Y.; Schlessinger, J. *Mol. Cell. Biol.* **1994**, *14*, 5192−5201.
(37) Keilhack, H.; Tenev, T.; Nyakatura, E.; Zimmermann, J. G.; Nielsen, L.; Seedorf, K.; Bohmer, F.-D. *J. Biol. Chem.* **1998**, *273*, 24839−24846.
(38) Ward, C. W.; Gough, K. H.; Rashke, M.; Wan, S. S.; Tribbick, G.; Wang, J.-X. *J. Biol. Chem.* **1996**, *271*, 5603−5609.
(39) Rojas, M.; Yao, S. Y.; Lin, Y.-Z. *J. Biol. Chem.* **1996**, *271*, 27456−27461.
(40) Ritter, C. L.; Arteaga, C. *Semin. Oncol.* **2003**, *30* (Suppl. 1), 3−11.
(41) (a) Hunter, T.; Sefton, B. *Proc. Natl. Acad. Sci. U.S.A.* **1980**, *77*, 1311−1315. (b) Hunter, T. *Cell* **1987**, *50*, 823−829. (c) Hubbard, M. J.; Cohen, P. *Trends Biochem. Sci.* **1993**, *18*, 172−177.

Materials (Spring Valley, NY). Titanium of 99.99% purity was obtained from PureTech (Brewster, NY). Tetraethylene glycol-terminated thiol (**EG4**; Figure 2) and the corresponding amine-terminated thiol (**EG4N**; Figure 2) as a hydrochloride salt were obtained from Prochimia (Gdansk, Poland).[42] The sulfosuccinimidyl 4-(*N*-maleimidomethyl)-cyclohexane-1-carboxylate (SSMCC) linker was obtained from Pierce Biotechnology (Rockford, IL). Nematic LC 4′-pentyl-4-cyanobiphenyl (5CB) was obtained from EM Industries (New York, NY) sold under the trademark name Licristal (K15). Triethanolamine (TEA) was obtained in 99% purity from Fisher.

Peptides were synthesized at the University of Wisconsin Biotechnology Center. The purity of the peptides was found to be >98%, as determined by analytical HPLC, and their integrity was confirmed by MALDI-TOF mass spectrometry. Monoclonal anti-phosphotyrosine IgG was obtained from Sigma-Aldrich. Ethanol (200 proof) was obtained from Aaper Alcohol (Shelbyville, KY) and purged with argon gas before use. Poly(dimethylsiloxane) (PDMS) elastomeric stamps were prepared using a Sylgard 184 silicone elastomer kit obtained from Dow Corning (Midland, MI). All other materials were obtained from Sigma-Aldrich unless otherwise noted.

Preparation of Gold Surfaces. Gold films (20 nm in thickness) deposited by physical vapor deposition at an oblique angle of incidence onto piranha-cleaned glass slides were prepared according to previously reported procedures.[33] The angle of deposition (θ_i, measured from the surface normal) was 49°. These gold films are semitransparent and were used in experiments described below that employ optical microscopy. Infrared spectroscopy and ellipsometric thickness measurements were performed using reflective gold films prepared by sequential deposition of 10 nm of Ti and 200 nm of Au onto silicon wafers (Silicon Sense, Nashua, NH) at normal incidence. All gold films were used within one week of preparation.

Formation of Patterned Monolayers. A PDMS elastomeric stamp with raised features (having dimensions of 2−3 mm width and 2−3 mm height) was cast from an aluminum master. The stamp was inked with a 2 mM ethanolic solution of hexadecanethiol (C16) and then gently dried using a stream of nitrogen gas. The stamp was placed into conformal contact with an obliquely deposited gold film for 10 s. Next, solutions containing mixtures of **EG4N** and **EG4** (1 mM total thiol concentration) were prepared using argon-purged ethanol. These solutions were stored under an argon atmosphere to prevent oxidation of the sulfhydryl functionality. Droplets of the **EG4N** and **EG4** solutions were applied to the gold films in the regions between the patterned C16 monolayers. The substrates were stored in a chamber saturated with ethanol vapor (to prevent droplet evaporation) for 18 h, rinsed with copious amounts of water and ethanol, and then gently dried under a stream of nitrogen gas.

Preparation of Patterned Peptide-Modified Array. The chemistry and detailed protocols used to attach the peptides to the mixed monolayers formed from **EG4** and **EG4N** (formed, as described above) are provided in our previous publications.[27,30,31] In brief, 2 mM solutions of the heterobifunctional linker SSMCC (in 0.10 M TEA−HCl buffer, pH 7.0) were deposited as droplets onto the mixed monolayers and incubated for 45 min. These surfaces were rinsed gently in water and dried under nitrogen gas. Solutions of cysteine-terminated EGFR peptide substrates (**pY1173** or **Y1173**, 250 μM) in 0.10 M TEA−HCl buffer, pH 7.0, were then applied as droplets. We used cysteine-terminated peptides as they site-specifically react with surface-immobilized maleimide groups introduced by using SSMCC.[27,31,43−45] The substrates were stored in a chamber saturated with water for 3 h. The choice of the 3-h reaction time was guided by previously published results.[27,31] Unreacted maleimide groups on the surface were quenched with 2-mercaptoethanol. These surfaces were rinsed (twice) with 0.10 M TEA−HCl buffer containing 0.1% v/v Triton-X 100 for 5 min, washed with water, and dried under nitrogen gas. As described below, we characterized these surfaces by PM-IRRAS and ellipsometry.

Protein Binding Studies Using EGFR Peptide Surfaces. Monoclonal anti-phosphotyrosine IgG in PBS + 0.05% v/v Triton-X 100 was applied to the peptide (**pY1173** or **Y1173**)-decorated surfaces for 1.5 h. The samples were stored in a chamber saturated with water. Following incubation, all samples were rinsed (3×) for 5 min in PBS + 0.1% v/v Triton-X 100, washed with water, and dried under a stream of nitrogen gas before use. Rinsing the surface with buffer containing surfactant was found to be effective for removal of weakly bound protein.

Ellipsometry. A Rudolph AutoEL ellipsometer (wavelength of 632 nm, 70° angle of incidence) was used to determine the optical thicknesses of the mixed monolayers formed from **EG4** and **EG4N**, the immobilized **Y1173** and **pY1173**, and surfaces to which antibody was bound. Ellipsometric constants were determined at five locations on each sample. As described previously, a simple slab model was used to interpret these constants. The slab was assumed to have an index of refraction of 1.46.[27]

Polarization-Modulation Infrared Reflection Absorption Spectroscopy. Infrared spectra of EGFR peptide substrates immobilized on gold films (thickness of 2000 Å) were recorded using a Nicolet Magna-IR 860 FT-IR spectrometer with photoelastic modulator (PEM-90, Hinds Instruments, Hillsboro, OR), synchronous sampling demodulator (SSD-100, GWC Technologies, Madison, WI), and a liquid nitrogen-cooled mercury cadmium telluride detector. All spectra were taken at an incident angle of 83° with the modulation centered at 1600 cm^{-1}. For each sample, 500 scans were taken at a resolution of 4 cm^{-1}. Data were collected as differential reflectance vs wave number, and spectra were normalized and converted to absorbance units via the method outlined in Frey et al.[46]

Assembly of Liquid Crystal Cells for Measurements of Anchoring Energies. The anchoring energies of the nematic liquid crystal 5CB on peptide-decorated surfaces incubated against antibody were measured by pairing the peptide-decorated surfaces with reference surfaces, as depicted in Figure 1. The reference surfaces were selected to strongly anchor the LC. As described previously, gold films deposited at an angle of incidence (θ_i) of 64° and treated with a 2 mM solution of pentadecanethiol (C15) for 2 h are suitable for use as reference surfaces.[31] The mutual orientations of the two surfaces were defined such that the in-plane direction of deposition of the gold film on the reference surface was rotated approximately 90° relative to that of the top surface (see arrows in Figure 1a). The two surfaces were spaced apart by a thin film of Mylar with a thickness of 12 μm. As described in detail in the Supporting Information (Figure S1), the Mylar film was placed along one edge of the paired surfaces so as to create a cavity between the two surfaces that varied in thickness from 12 μm at one edge to contact at the other. The cavity was filled with 5CB heated to approximately 40 °C (above the clearing temperature for 5CB). We measured the optical properties of the LC film after approximately 30 min of cooling the 5CB to room temperature (22 °C), as both temperature[47] and age of the sample (surface gliding)[32] have been reported in some circumstances to influence the measured anchoring strength.

Optical Measurements for Determination of Anchoring Energies. The approach reported in this article for measurement of the azimuthal anchoring energy of peptide-decorated interfaces is a variant of the so-called torque balance method.[29,32] For films of LC that are sufficiently

(42) Pale-Grosdemange, C.; Simon, E. S.; Prime, K. L.; Whitesides, G. M. *J. Am. Chem. Soc.* **1991**, *113*, 12−20.
(43) Matsuzawa, M.; Umemura, K.; Beyer, D.; Sugioka, K.; Knoll, W. *Thin Solid Films* **1997**, *305*, 74−79.
(44) Xiao, S.-J.; Textor, M.; Spencer, N. D. *Langmuir* **1998**, *14*, 5507−5516.
(45) Houseman, B. T.; Gawalt, E. S.; Mrksich, M. *Langmuir* **2003**, *19*, 1522−1531.
(46) Frey, B. L.; Robert, M. C.; Weibel, S. C. In *Handbook of Vibrational Spectroscopy;* Griffiths, P. R., Ed.; Wiley & Sons: New York, 2002; Vol. 2; p 1042.
(47) Iimura, Y.; Kobayashi, N.; Kobayashi, S. *Jpn. J. Appl. Phys., Part 1* **1995**, *34*, 1935−1936.

thin, the elastic bulk torque of a LC with a twist distortion (twist angle ψ) competes with the surface anchoring torque such that the equilibrium position of the director η_d deviates by an angle (φ) from the easy axis η_o (Figure 1). The azimuthal anchoring energy is calculated from measurements of ψ and φ as

$$W = \frac{2K_{22}\Psi}{d\sin(2\varphi)} \quad (1)$$

where K_{22} is the twist elastic constant for the LC, and d is the thickness of the film of LC. The optical methods used to measure the local thickness (d) of the LC, the angle over which the LC forms a twist (ψ), and the angle of deviation of the director from the easy axis (φ) are described in detail in a previous publication[29] and were adapted from a report by Fonseca and Galerne.[32,48] A discussion of the assumptions underlying the use of eq 1 can be found in a prior publication.[29] Here, we mention that these measurements were performed using a polarized light microscope (BX 60, Olympus) equipped with an X−Y translation stage and a digital camera for image capture. Consistent settings of both the microscope light source (aperture set at one-half maximum, and lamp intensity also set at one-half maximum), digital camera (2.8 f-stop, 1/200 shutter speed), and optical zoom 4× allowed the direct comparison of images obtained using different samples. To quantify the luminosity of the LC in contact with the surfaces, each image was converted to gray scale. The average pixel brightness of a region was calculated, and we assigned a completely black pixel the value of 0 and a completely white pixel the value of 255.

Results and Discussion

Preparation and Characterization of Peptide-Modified Interfaces. To confirm covalent attachment of **Y1173** and **pY1173** peptides to the mixed SAMs formed from **EG4** and **EG4N** and to provide independent evidence for specific binding of the anti-phosphotyrosine antibody to the surfaces presenting **pY1173** but not **Y1173**, we employed a combination of infrared spectroscopy and ellipsometry. These measurements were performed using SAMs prepared from a series of ethanolic solutions containing different mixtures of **EG4** and **EG4N** (1, 5, 10, 25, 50, and 100 mol % **EG4N**; total thiol concentration of 1 mM), as described in the Materials and Methods. Infrared spectra obtained by using PM-IRRAS confirmed that treatment of these mixed SAMs with the heterobifunctional linker SSMCC led to attachment of the maleimide group of SSMCC to the amino functionality of **EG4N**. Specifically, strong absorption bands were observed for the maleimide asymmetric (1707 cm^{-1}) and symmetric (1745 cm^{-1}) stretching modes (Supporting Information, Figure S3). In addition, consistent with the expectation that the reaction of SSMCC with the SAM generates an amide bond, we observed a band in the 1655 cm^{-1} region corresponding to the Amide I (C═O) stretching mode.[49] Infrared spectra of the SSMCC-activated mixed SAMs subsequently treated with cysteine-terminated EGFR peptides (250 μM of **Y1173** or **pY1173**) provided evidence for immobilization of the peptides, as characteristic Amide I (1670 cm^{-1}) and Amide II (1537 cm^{-1}) bands were observed for both peptides,[44,49] as was the loss of the peak at 1745 cm^{-1} (maleimide symmetric stretching mode) because of breaking of molecular symmetry upon formation of the covalent adduct. Systematic changes in the intensity of the amide bands with composition of the mixed SAM also served to demonstrate control over the density of peptides immobilized at these surfaces (Figure S3).

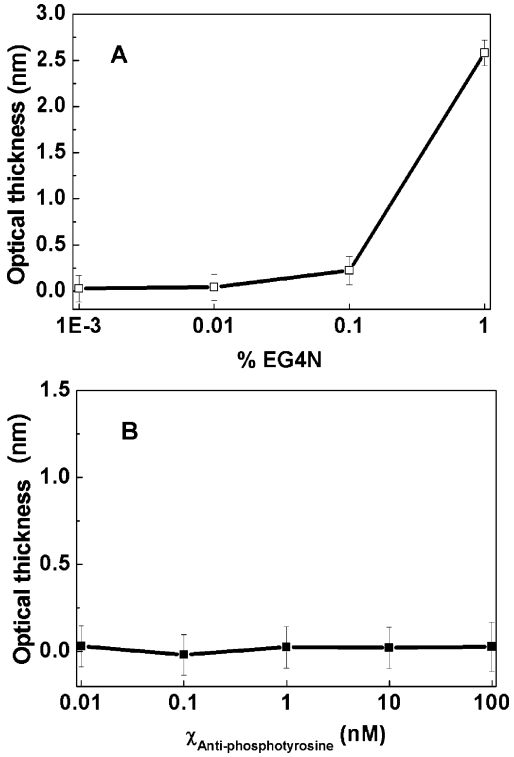

Figure 3. Ellipsometric thickness measurements. (A) Optical thickness of antibody bound to surfaces prepared by immobilizing **pY1173** to SAMs containing 0.001, 0.01, 0.1, and 1% **EG4N**. The concentration of antibody was 100 nM. (B) Optical thickness of antibody bound to surfaces presenting **pY1173** (0.001% **EG4N**) that were incubated in solutions containing 0.01, 0.1, 1.0, 10, and 100 nM antibody in PBS + 0.05% Triton X 100 buffer. $\chi_{Anti-phosphotyrosine}$ = concentration of monoclonal anti-phosphotyrosine (IgG) in nM.

Measurements of the ellipsometric thicknesses of the mixed SAMs provided further evidence for formation of surfaces decorated with controlled densities of peptides. The maximum contribution of each peptide to the ellipsometric thickness of the interface was 0.70 nm, independent of the phosphorylation status of the peptide (**Y1173** versus **pY1173**). We also used ellipsometry to confirm binding of the anti-phosphotyrosine antibody to the surfaces decorated with **pY1173**, as a function of the density of peptide on the surface (Figure 3A). For surfaces prepared using 1% **EG4N** to immobilize **pY1173**, the ellipsometric thickness increased by 2.6 ± 0.1 nm following incubation with 100 nM antibody. Within the error of measurement, no change in optical thickness (0.20 ± 0.2 nm) was observed on the **Y1173**-modified surface after treatment with the monoclonal anti-phosphotyrosine IgG (100 nM) or for the **pY1173**-modified surface when the percentage of **EG4N** used to form the mixed SAM was <0.1% (Figure 3A). These results, when combined, confirm selective binding between the phospho-specific antibody and the immobilized phosphorylated EGFR peptide sequence (**pY1173**).

Here we mention that we also performed ellipsometric measurements on surfaces prepared using 0.001% **EG4N,** following immobilization of **pY1173** and treatment with varying amounts of antibody (10 pM to 100 nM). As shown in Figure 3B, ellipsometry is not sufficiently sensitive to permit detection of anti-phosphotyrosine IgG bound to these surfaces when using concentrations of antibody between 10 pM and 100 nM. Below,

(48) Polossat, E.; Dozov, I. *Mol. Cryst. Liq. Cryst.* **1996**, *282*, 223−233.
(49) Frey, B. L.; Corn, R. M. *Anal. Chem.* **1996**, *68*, 3187−3193.

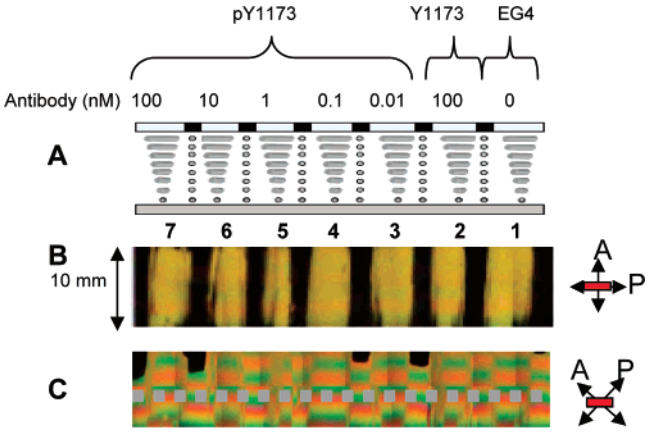

Figure 4. (A) Schematic representation of optical cell prepared from a surface patterned with peptides and incubated with antibody (top) and a reference plate (bottom) (see text for details). (B) Polarized light micrograph of the array shown in (A) when viewed with polarizer and analyzer perpendicular to each other (as indicated: A, analyzer; P, polarizer). (C) When both polarizers were rotated to 45° with respect to the sample. Gray dotted line indicates the position (constant thickness $d = 6.0 \pm 0.5\ \mu$m, as determined from the Michel-Levy chart) at which all angular measurements were made (see text).

Table 1. Measured Angles and Calculated Anchoring Energies Reported as a Function of Antibody Concentration; See Text for Details

region	peptide + antibody (nM)	γ (deg)	δ (deg)	φ (deg)	ψ (deg)	W (μJ/m^2)
1	**EG4**	164.9	84.9	9.9	74.9	5.3
2	**Y1173** + 100	163.6	83.7	10.1	73.6	5.19
3	**pY1173** + 0.01	161.8	83.4	11.6	71.8	4.43
4	**pY1173** + 0.1	159.4	81.6	12.2	69.4	4.09
5	**pY1173** + 1.0	153.5	81.3	17.8	63.5	2.65
6	**pY1173** + 10	145.3	78.8	23.5	55.3	1.81
7	**pY1173** + 100	139.9	78.3	28.4	49.9	1.43

we report that measurements of anchoring energies of LCs are sufficiently sensitive to report specific binding of the antibodies to these surfaces.

Measurement of Anchoring Energies. We chemically patterned gold films deposited at an angle of 49° so as to permit simultaneous measurement of anchoring energies of LCs on seven regions of the surface. We refer to the seven regions of the gold film that were defined by microcontact-printed hexadecanethiol as Regions 1−7 (Figure 4). Mixed monolayers comprising 0.01 μM **EG4N** and 1 mM **EG4** (i.e., 0.001% **EG4N**) were formed on Regions 2−7, and a monolayer of **EG4** was prepared on Region 1. Regions 2−7 were subsequently activated with SSMCC and reacted with **pY1173** (Regions 3−7) or **Y1173** (Region 2) as described above. Regions 3−7 presenting **pY1173** were treated with solutions containing either 0.01, 0.1, 1, 10, or 100 nM of anti-phosphotyrosine antibody (in PBS + 0.05% Triton-X 100 buffer), respectively (Table 1), and control Region 2 presenting **Y1173** was treated with 100 nM anti-phosphotyrosine antibody.

To measure the anchoring energies of nematic 5CB on the above-described surfaces, we paired the antibody-treated peptide array with the reference surface and subsequently filled the wedge-shaped cavity between the two surfaces with the 5CB (see Materials and Methods for details). Figure 4B shows the optical appearance of the sample imaged using a polarized light microscope (crossed polars). The dark vertical bands in the image in Figure 4B correspond to the regions of microcontact printed C16 that separate the peptide-decorated regions labeled 1−7. The LC in contact with the C16-printed regions appears dark because the orientation of the easy axis of the LC on the C16-printed surface coincides with the orientation of the easy axis of the LC on the reference surface. Under these conditions, when the easy axes of the surfaces are parallel to either the polarizer or analyzer (as shown in Figure 4B), there is no change in the polarization of light passing through the LC, and thus the LC appears dark between crossed polars.

The **EG4** (Region 1) and peptide-decorated regions of the surface (Regions 2−7) lie between the dark bands defined by the hexadecanethiol. The LC in contact with Region 1 is largely bright in appearance when viewed between crossed polars, with the exception of the lower edge (Figure 4B), which is darker. Rotation of the analyzer by approximately 90° (parallel polars) resulted in the near extinction of light passing through the previously bright regions of Region 1: the previously dark lower edge turned bright (result not shown). These two results, when combined, indicate that the LC assumed a twist distortion in most of Region 1 because of the near-orthogonal orientations of the easy axes of the LC on the two confining surfaces (Figure 4A). The lower edge of the image in Figure 4A corresponds to the part of the optical cell where the peptide-decorated surface and reference surface come into near contact (see Materials and Methods). In this region, the strength of anchoring of the LC on the **EG4** surface is not sufficient to orient the LC along the easy axis of the **EG4** surface and thus induce a twist distortion of the LC. This situation arises because the torque exerted on a surface by a twist distortion increases with the reciprocal of the thickness of the film of LC.[32] The darker areas at the bottom of Region 1 thus correspond to regions of LC that are largely oriented (with little distortion) along the easy axis of the reference surface.

Regions 2−7 appear qualitatively similar to Region 1 (that is, bright in appearance) when viewed between crossed polars (Figure 4B). Close inspection, however, reveals two important differences. First, it is apparent that dark bands have formed at the edges of Regions 2−7 that are near the microcontact printed regions of C16. These dark regions correspond to the location of the edges of the droplets of antibody solutions that were incubated on the peptide-decorated surfaces. A range of complex physical processes are known to occur at the edges of droplets of protein solutions placed onto surfaces, including processes of adsorption and drying associated with evaporation of water.[50] These processes give rise to changes in the structure of the surface that result in a substantial decrease in anchoring energy and decrease in the twist angle of the LC. We avoided those edge regions in our analysis of the optical images leading to estimates of anchoring energies. Second, and more importantly, close inspection of Regions 2−7 (away from edges) reveals that there is a systematic decrease in the brightness of the image as a function of increasing antibody concentration (0.01, 0.1, 10, 100 nM of anti-phosphotyrosine antibody). When viewed between crossed polars at low magnification, the effect is relatively subtle to the naked eye, but it can be readily seen in higher resolution images of Regions 3−7 (obtained from regions of the optical cell with a thickness of LC of $6.0 \pm 0.5\ \mu$m; see below) shown in Figure 5. These differences in optical appear-

(50) (a) Balagurunathan, Y. *J. Biomed. Opt.* **2004**, *9*, 663−678. (b) Balagurunathan, Y.; Dougherty, E. R. *J. Biomed. Opt.* **2002**, *7*, 507−523.

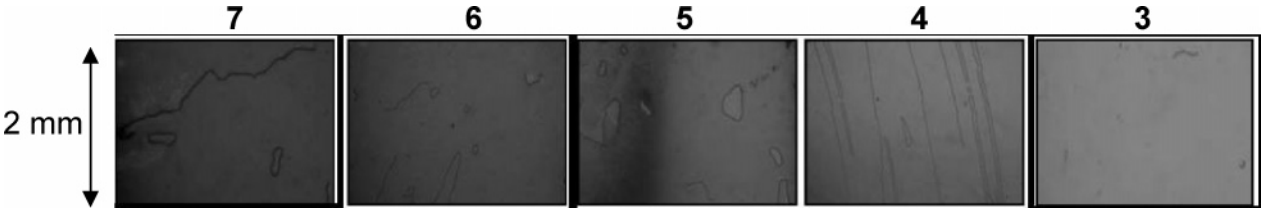

Figure 5. High-resolution optical images (crossed polars) of Regions 3−7 shown in Figure 4.

ance of the LC indicate the orientation of the LC is changing on the **pY1173**-decorated surfaces as a function of the concentration of antibody. As revealed below, rotation of the analyzer reveals that the twist angle of the LC decreased across Regions 3−7 (i.e., with increasing antibody concentration) because of a decrease in the anchoring energy of the LC on the **pY1173**-decorated surfaces incubated with antibody.

Optical measurements to quantify the orientation of the LC in Regions 1−7 were performed at locations where the thickness of the film of LC between the peptide-decorated surfaces and reference surface was 6.0 ± 0.5 μm, as determined by comparing the interference colors shown in Figure 4C to those observed in a Michel-Levy chart.[51] Inspection of eq 1 reveals that knowledge of the twist angle (ψ) and deviation angle (φ) at the peptide-decorated surfaces is required for evaluation of the anchoring energy of the LC. These angles were calculated from the experimentally determined angles γ and δ (Figure 1). The details of the methods used to determine these angles can be found in the Supporting Information. Briefly, the sample was held at a fixed position on the microscope stage, and the analyzer was rotated to an orientation such that the intensity of light transmitted through the analyzer was reduced to a minimum. Under these conditions, the angle formed between the analyzer and source polarizer is equal to γ.[29,32] To determine the position of the analyzer that corresponded to the minimum in the intensity of transmitted light, we captured optical images of the LC at regularly spaced intervals of the analyzer orientation. Image processing (Adobe Photoshop) was used to determine the mean luminosity of the twisted domain of the LC. We plotted the mean luminosity of images captured as a function of analyzer position, as shown in Figure 6A. The intensity of transmitted light, according to the optical behavior of twisted LCs in the waveguide region, should follow the function $f(x) = \cos^2(x)$, where x is the angle of the analyzer.[32] Inspection of Table 1 reveals that the angle between the polarizer and analyzer (γ) varied monotonically from 163.6° for Region 2 (**Y1173** incubated with 100 nM of anti-phosphotyrosine antibody) to 139.9° for Region 7 (**pY1173** incubated with 100 nM anti-phosphotyrosine antibody). A similar analysis was carried out to find δ, the relative orientation of the easy axes of the LC on the two surfaces (Figure 6B). Inspection of Table 1 shows that only a modest change in δ occurs across the sample. This variation is largely due to spatial variation in the azimuthal angle of incidence of the gold during deposition of the gold films onto the glass microscope slides (as discussed in ref 30). It is important to point out that the anchoring energy is an intrinsic property of the interface, and accurate values of anchoring energies can therefore be obtained using surfaces across which the angle δ varies in a known manner.

(51) More recent versions of the Michel-Levy chart can be found at the Olympus website. http://www.olympusmicro.com (accessed April 2007).

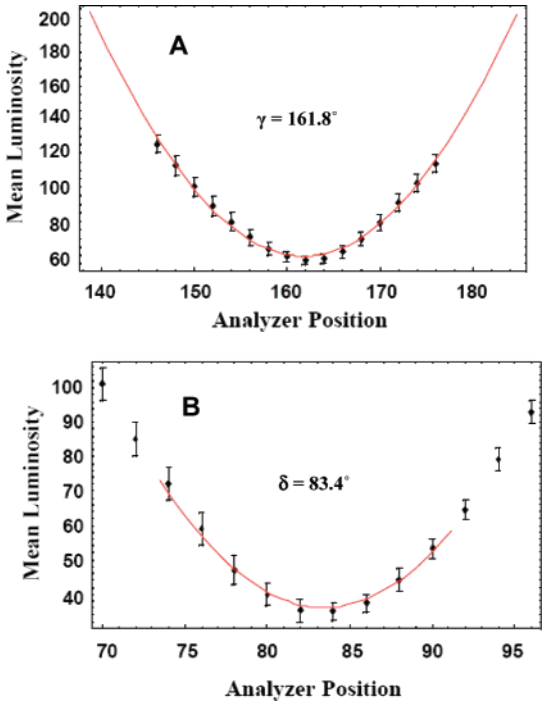

Figure 6. Illustration of optical method used to determine angles γ and δ for evaluation of anchoring energy. The data were obtained from Region 3 of the sample shown in Figure 4B. See text for details and Figure S6 for corresponding polarized light images.

The angle diagram used to identify ψ and φ from the experimentally measured parameters δ and γ is shown in Figure 1.[29,32] These relationships, when combined with the known twist elastic constants of 5CB ($K_{22} = 4.22 \pm 0.5$ pN) and eq 1, permit evaluation of the anchoring energy (Table 1). Inspection of Table 1 reveals that the anchoring energy on the **EG4**-decorated surfaces is 5.3 μJ/m^2, in good agreement with previous reports.[29] On these **EG4**-decorated surfaces, the torque generated by the twist distortion causes the orientation of the LC to deviate from the easy axis by 9.9°. Figure 7 shows that this angle increases to 28.4° when the **pY1173**-decorated surfaces are incubated with 100 nM anti-phosphotyrosine antibodies. To quantify the experimental error involved in these measurements, on an independently prepared surface, we treated each of the Regions 3−7 with 0.1 nM anti-phosphotyrosine antibody (Table S1 of Supporting Information). From these measurements, a standard error of the mean ($n = 5$) was calculated to be ±0.5° (as indicated by the error bars in Figure 7). The corresponding standard error in calculated values of anchoring energies was 0.3 μJ/m^2 (Table S1, error bars in Figure 8).

Immobilization of **Y1173** and incubation in 100 nM anti-phosphotyrosine leads to an anchoring energy of 5.2 μJ/m^2 (Table 1), a value that is not significantly different from that of the **EG4**-terminated surface (5.3 μJ/m^2). In contrast, incubation of the surfaces presenting **pY1173** with increasing concentra-

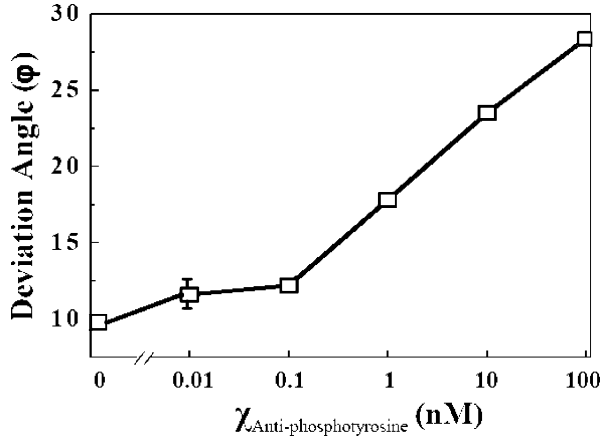

Figure 7. Deviation of orientation of LC from easy axis (φ) plotted as a function of antibody concentration in solution.

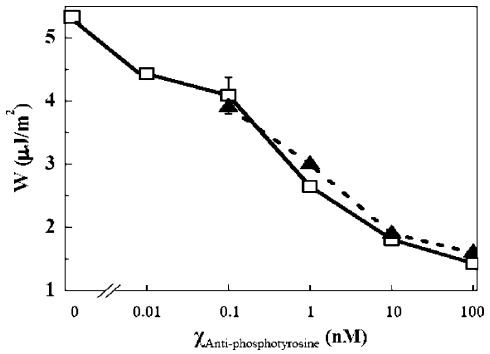

Figure 8. Anchoring energy (W) of LC as a function of concentration of monoclonal anti-phosphotyrosine antibody (IgG). Two independent data sets are shown, along with the standard error calculated from five repeat measurements at 100 pM antibody.

tions of anti-phosphotyrosine antibody leads to a systematic decrease in anchoring energy to 1.4 μJ/m^2 (data indicated with open squares in Figure 8 correspond to data presented in Figure 7). Figure 8 reveals a weakly sigmoidal relationship between anchoring energy and logarithm of the concentration of antibody in solution that extends over 4 orders of magnitude of antibody concentration. An important observation is that a concentration of phospho-specific antibody of 10 pM leads to an anchoring energy of 4.1 μJ/m^2 on surfaces presenting **pY1173**, a value that is significantly lower than that measured when 100 nM antibody is incubated against the surface presenting **Y1173** (5.2 μJ/m^2). Finally, we note that Figure 8 also shows a second data set (solid triangles, 100 pM to 100 nM antibody) that was obtained using an independently prepared surface. Good agreement between independently prepared surfaces is evident.

The above-described measurements of anchoring energies of liquid crystals on peptide-patterned surfaces incubated against subnanomolar concentrations of anti-phosphotyrosine antibody are interesting in light of our past observations regarding the use of LCs to detect the presence of proteins bound at surfaces.[22−25,31] Our previous measurements focused on characterizing spontaneous changes in the easy axis of LCs induced by captured proteins and revealed that the orientations of LCs typically become nonuniform on surfaces that present increasing amounts of bound protein.[22−25,31] The approach reported herein contrasts with our past work in that it does not require a bound protein to induce a change in the easy axis in order to be reported by the LC. Specifically, the measurements reported in this article show that LCs can be used to report the presence of low concentrations of antibodies captured on surfaces via measurement of anchoring energies that change systematically with incremental increase in the concentration of the antibody. From these combined results, we draw an important conclusion: that in the case of proteins bound at surfaces, a measurable and systematic reduction in anchoring energy caused by captured protein precedes a spontaneous change in orientation of the LC (that is, a change in the orientation of the easy axis). The measurement of anchoring energy provides, therefore, a means to increase the sensitivity of methods based on LCs for amplifying and detecting proteins at interfaces. We also note that the results reported in this article indicate that measurements of anchoring energies of LCs also provide a dynamic range of measurement that extends over 4 orders of magnitude of antibody concentration.

Inspection of Figures 3 and 7 reveals that the amounts of bound antibody that lead to changes in anchoring energy are sufficiently small that they do not lead to measurable changes in ellipsometric thicknesses. Control experiments described above confirm that the changes in anchoring energy come about because of specific binding events. We have estimated an *upper bound* on the mass density of antibody that leads to measurable changes in anchoring energies of LCs on these surfaces by assuming that (i) the mole fraction of **EG4N** in the mixed monolayer is the same as the solution composition, (ii) all amine-terminated thiols within the mixed monolayer react to immobilize one EGFR peptide molecule, and (iii) one antibody molecule is bound to each peptide molecule on the surface. Using these assumptions, we calculate that the anchoring energy of the LC on the surface exposed to 100 nM antibody (which is the highest concentration used in our study) is influenced by <1 ng/cm^2 of captured antibody. We emphasize that this mass density corresponds to the maximum concentration investigated in our study (100 nM), and that much lower concentrations of antibody (0.01 nM) lead to measurable changes in anchoring energies of the LCs. On surfaces exposed to 0.01 nM antibody, we expect the mass densities of antibody to be $<<1$ ng/cm^2. These results lead us to conclude that methods based on measurements of anchoring energies of LCs can likely be made to be more sensitive than other label-free methodologies used to measure biomolecular binding events and/or surface adsorption phenomena, including surface plasmon resonance spectroscopy ($\sim$2 ng/cm^2),[52] optical waveguide light mode spectroscopy ($\sim$1 ng/cm^2),[53] and attenuated total reflection infrared absorption spectroscopy ($\sim$1 ng/cm^2).[54]

Conclusion

The main conclusion of the study presented in this article is that measurements of the energy of interaction of LCs with surfaces provide simple and sensitive methods to quantify proteins captured on surfaces through interactions with immobilized ligands. To our knowledge, this study provides the first demonstration that anchoring energies of LCs can be used to report protein-binding events at surfaces. Concentrations of

(52) Whalen, R. J.; Wohland, T.; Neumann, L.; Huang, B.; Kobilka, B. K.; Zare, R. N. *Anal. Chem.* **2002**, *74*, 4570−4576.
(53) Bearinger, J. P.; Voros, J.; Hubbell, J. A.; Textor, M. *Biotechnol. Bioeng.* **2003**, *82*, 465−473.
(54) Rigler, P.; Ulrich, W.-P.; Hoffman, P.; Mayer, M.; Vogel, H. *ChemPhysChem* **2003**, *4*, 268−275.

antibodies in the 10 pM to 100 nM range were reported upon binding to EGFR peptides presented at surfaces. The method relies on measurement of the response of a LC in contact with a surface presenting captured proteins to an applied perturbation. In this study, a twist distortion is generated so as to apply a mechanical torque to LCs. Other methods of perturbing the LC can be envisaged, including the use of applied electric fields. The potential merits of the principles reported in this article include sensitivity (10 pM in antibody concentration), dynamic range (4 orders of magnitude), and ability to perform multiplexed assays on a single surface (image surfaces with patterned analytic zones). Such characteristics lead us to believe that the principles described in this article may be broadly useful for the analysis of proteins and other biomolecules involved in interactions that regulate a range of complex and poorly understood chemical and biological events.

Acknowledgment. This research was partially supported by the National Science Foundation (DMR 0079983) and the National Institutes of Health (CA108467 and CA105730).

Supporting Information Available: Additional experimental procedures for anchoring energy measurements, characterization data for peptides and proteins immobilized on gold surfaces such as infrared spectra and ellipsometric measurements. This material is available free of charge via the Internet at http://pubs.acs.org.

JA073203X